N O T I C E

THIS DOCUMENT HAS BEEN REPRODUCED FROM MICROFICHE. ALTHOUGH IT IS RECOGNIZED THAT CERTAIN PORTIONS ARE ILLEGIBLE, IT IS BEING RELEASED IN THE INTEREST OF MAKING AVAILABLE AS MUCH INFORMATION AS POSSIBLE

DRD Line No. SE-5

JPL NO. 9950-604 DOE/JPL 955688-80/3

Distribution Category UC-63

(NASA-CR-165043) DEVELOPMENT OF AN ALL-METAL THICK FILM COST EFFECTIVE METALLIZATION SYSTEM FOR SOLAR CELLS Quarterly Report, Nov. 1980 - Apr. 1981 (Ross (Bernd) Associates) 40 p HC A03/MF A01

N82-14630

Unclas

G3/44 08471

DEVELOPMENT OF AN ALL-METAL THICK FILM COST EFFECTIVE METALLIZATION SYSTEM FOR SOLAR CELLS

BERND ROSS

BERND ROSS ASSOCIATES
2154 Blackmore Ct.
San Diego, CA 92109

QUARTERLY REPORT NO. 3
Nov. 1980 - April 1981

SEPTEMBER 1981

Contractual Acknowledgement

The JPL Low-Cost Silicon Solar Array Project is sponsored by the U.S. Department of Energy and forms part of the Solar Photovoltaic Conversion Program to initiate a major effort toward the development of low-cost solar arrays. This work was performed for the Jet Propulsion Laboratory, California Institute of Technology by agreement between NASA and DOE.

DRD Line No. SE-5 DOE/JPL-955688-80/10
Distribution Category UC-63

DEVELOPMENT OF AN ALL-METAL THICK FILM COST EFFECTIVE METALLIZATION SYSTEM FOR SOLAR CELLS

BERND ROSS

BERND ROSS ASSOCIATES
2154 Blackmore Ct.
San Diego, CA 92109

QUARTERLY REPORT NO. 3
Nov. 1980 - April 1981

SEPTEMBER 1981

Contractual Acknowledgement

The JPL Low-Cost Silicon Solar Array Project is sponsored by the U.S. Department of Energy and forms part of the Solar Photovoltaic Conversion Program to initiate a major effort toward the development of low-cost solar arrays. This work was performed for the Jet Propulsion Laboratory, California Institute of Technology by agreement between NASA and DOE.

"This report was prepared as an account of work sponsored by the United States Government. Neither the United States nor the United States Department of Energy, nor any of their employees, nor any of their contractors, subcontractors, or their employees, makes any warranty, express or implied, or assumes any legal liability or responsibility for the accuracy, completeness or usefulness of any information, apparatus, product or process disclosed, or represents that its use would not infringe privately owned rights."

TABLE OF CONTENTS

Section	Titles	Page
	Table of Contents	i
	List of Illustrations and Tables	ii
1.0	Summary	1
2.0	Introduction	2
3.0	Paste and Contact Experimentation, Carbon Fluoride	3
4.0	Paste and Contact Experimentation, Silver Fluoride	13
5.0	Results of Analysis	21
6.0	Information Exchange with German R&D Labs and PVSEC	29
7.0	Conclusions and Problems	31
8.0	Plans and Recommendations	33
9.0	References	34
10.0	Progress on Program Plan	35

List of Illustrations and Tables

Figure		Page
1	Photograph of test pattern	4
2	SEM micrograph of F7 copper fluorocarbon electrode at 1800x	6
3	SEM micrograph of F7 copper fluorocarbon electrode at 9000x	6
4	SEM micrograph of F13 copper fluorocarbon electrode at 1800x	11
5	SEM micrograph of F13 copper fluorocarbon electrode at 9000x	11
6	SEM micrograph of substrate under F13 electrode at 1800x	11
7	SEM micrograph of substrate under F13 electrode at 9000x	11
8	Photographs of 3 paste electrodes with Scotch tape test above	14
9	SEM micrograph of S032 silver electrode at 1800x	15
10	SEM micrograph of S032 silver electrode at 9000x	15
11	SEM micrograph of F12 copper silver fluoride nitrogen fired print at 1800x	17
12	SEM micrograph of F12 copper silver fluoride nitrogen fired print at 9000x	17
13	SEM micrograph of F15 flake copper electrode print at 1800x	18
14	SEM micrograph of F15 flake copper electrode print at 9000x	18
15	Optical micrograph composite of S080 successful and S079 unsuccessful pastes	22
16	SEM optical micrograph composite of S080 unsuccessful substrate and electrode	24
17	SEM optical micrograph composite of S080 successful substrate and electrode	25
18	Xray dispersive spectrum of successful S080 electrode	26
19	Xray dispersive spectrum of successful S080 substrate	27

Table		
I	Composition of Paste F13	9
II	Two step firing process	10

1.0 Summary

Experiments were conducted with variations in paste parameters, firing conditions, including gas ambients, furnace furniture, silicon surface and others.

The Photovoltaic Solar Energy Conference was attended and a paper was presented. Semiconductor and solar cell research activities in Munich were visited and activities of mutual interest were discussed.

A liquid medium, intended to provide transport during the carbon fluoride decomposition was incorporated in the paste with promising results.

2.0 Introduction

The purpose of this study is to provide economical, improved thick film solar cell contacts for the high-volume production of low-cost silicon solar array modules for the LSA Project.

This work is based upon the concept of an all-metal screenable electrode ink, investigated in Contract #955164. It was first found that silver powder with lead acting as a liquid sintering medium and with silver fluoride acting as an oxide scavenger, continuous adherent electrode layers result on silicon. During the final phase of the antecedent contract it was shown that base metals such as copper can likewise be sintered to provide an ohmic contact on silicon when appropriately doped. The most successful screened solar cell contacts were achieved using germanium-aluminum and silicon-aluminum eutectics as additions to the pastes for back contacts.

The objectives of the investigation are to provide all-metal screenable pastes using economical base metals, suitable for application to low-to-high conductivity silicon of either conductivity type and possibly to aluminum surfaces.

3.0 Paste and Contact Experimentation, Carbon Fluoride

During the present interval paste formulation was reinstated at a new subcontract facility. The purpose of this change was to allow more intimate control of material and process by direct contract personnel.

New screens were designed and fabricated in order to allow utilization of convenient and economical 2cm x 2cm solar cell blanks. A design was made for a universal test pattern and solar cell front and back electrodes. These could be used both for basic ink parameter measurements and solar cell contact experimentation. The test pattern allows measurement of contact resistance, line resistance substrate resistivity, optical line resolution and electrical line resolution and is shown in Figure 1. The linear pattern at the top facilitates a measurement allowing the calculation of contact resistance (in Ωcm^2), simultaneously giving the resistivity of the silicon substrate. The large squares (2.5mm x 2.5mm), at the extremes of the linear array, provide the current electrodes in the measurement, while the small series of rectangles provide the voltage sources in the array. This portion of the design had been used previously[1]. A long line at the periphery of the pattern was used for measurement of the electrode resistance, from which the resistivity can be derived by

$$\rho = R \frac{tw}{\ell} \ \Omega cm \qquad (1)$$

where
$\rho \equiv$ electrode resistivity Ωcm
$R \equiv$ measured resistance, Ω
$t \equiv$ electrode thickness, cm
$w \equiv$ electrode width, cm
$\ell \equiv$ electrode length, cm

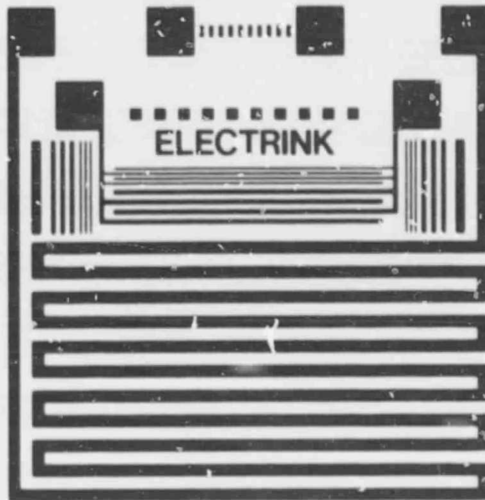

3X Actual Size

Figure 1. Photograph of screen pattern, with contact resistance, line resistance optical and electrical resolution test.

3.0 Cont.

The interwoven pattern under the contact resistance array serves to determine line definition and the degree of measureable crossover or bridging, based upon a resistance measurement. It will be noted that two sets of line pairs are provided, one that is coarse (.009 inches line width and spacing) and one that is fine, .004 inches line width and spacing (See Figure 1, lower and upper portion, respectively). It has been noted that screening in a direction perpendicular to a line tends to reduce line resolution. Based upon these designs, frames were ordered both for #325 mesh screens and #230 mesh screens. The #325 mesh screens were chosen initially to allow ultimate resolution, but proved to be too fine to allow sufficiently thick deposits. The #230 mesh screens were adequate.

Initial experiments with fluorocarbon pastes gave unsatisfactory results, both from an adhesive and a sintering standpoint. Figures 2 and 3 show an example of an electrode which exemplifies the problem. Microscopic examination of the lead raw material showed that a high percentage of the grains were quite large ($\sim 50 \mu m$), resulting both in poor distribution of the liquid sintering medium, as well as the possibility of the printing screen acting as a sieve. This would hold back a portion of the lead component, upsetting the intended compositional ratios, and could explain the problem of undersintering.

ORIGINAL PAGE IS
OF POOR QUALITY

Figure 2. SEM micrograph at 1800x of F7 copper fluorocarbon paste fired at 600°C by the two step process.

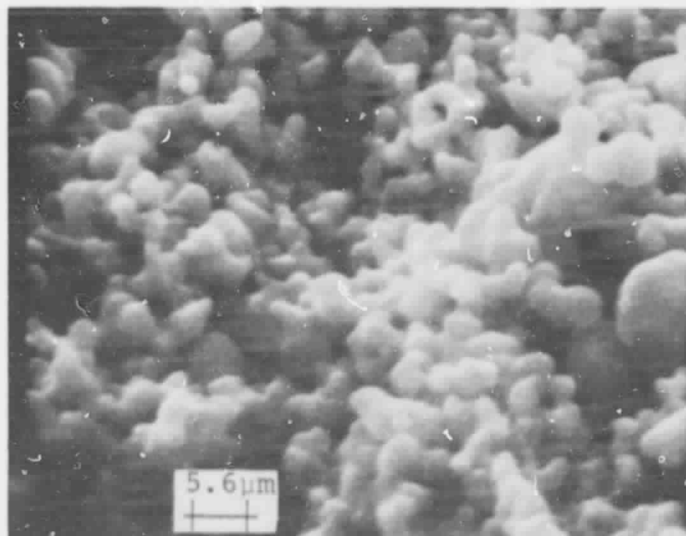

Figure 3. Same as above except 9000x. Note lack of sintering as shown by small particle size and absence of contiguous grain aggregates.

3.0 Cont.

This problem was eliminated by ordering #200 lead powder, and sifting the available powder through a #400 stainless steel screen. Some improvement in sintering resulted from this procedure, however the adhesion problem remained.

In addition to problems with excessive particle size in lead, copper powder from suppliers other than Colorial Metal Corporation also had too large a particle size distribution (large particle diameters). However, the most recent batch of copper received from Colonial Metals Corporation was below specifications for particle size and gave problems with a) the amount of powder that could be accommodated by a given quantity of vehicle (metal content) and b) the apparent "fluffiness" of the metal powder. Both a) and b) are attributable to smaller than usual particle diameters.

A total of 99 different paste formulations were manufactured by the previous subcontractor, including many attempts to reproduce S071, S079 and S080 which represented the best solar cell electrodes made to date (previous contract #955164)[2]. It was deemed appropriate to start over numbering pastes manufactured by the new subcontractor, beginning with F1 (which would have been S100 under the old scheme).

The first fluorocarbon ink in this series was F4 utilizing 0.7 wt% fluorocarbon powder with the results described above.

3.0 Cont.

Pastes were produced with various copper powders including copper flake (see next section), without a marked improvement. Fluorocarbon content was varied from 0.7 wt% (F4) to 2.1 wt% (F11) with the medium range (1.0 to 1.2 wt%) yielding the best results to date.

An extensive analysis was undertaken by Dr. Joseph Parker, of the possible chemical reactions of the paste constituents throughout the thermal history of the screened electrodes. A set of simple equations was written and the thermochemical analysis was done, based upon heats of reaction from published or derived heats of formation, for the various compounds. The numerical value and algebraic signs of the heats of formation indicate the likelihood that certain reactions should be emphasized or reduced in quantity. Subsequently it was desirable to verify these clues by direct experimentation and further physical analysis with differential thermal analysis (DTA) and thermal gravimetric analysis (TGA).

The above analysis showed that it would be desirable to provide an additional liquid medium, whose function was to promote contact between the copper powder grains and the freshly exposed silicon surface, during the scavenging activity of the fluorine from the fluorocarbon source. Earlier work with silver fluoride had shown that the fluorine scavenging activity takes place very rapidly ($\sim$1 sec), while the silver fluoride salt is in a liquid form. The reaction

3.0 Cont.

products, solid silver metal and gaseous silicon tetrafluoride, as well as water, drive the reversible reaction in one direction through the mass action law, and the contact between silver and silicon is a consequence of the reaction site. Contact between the copper grains and the silver fluoride is promoted by the liquid lead (liquid phase sintering medium), during the longer term of the sintering step. In the case of the fluorocarbon decomposition the reaction proceeds without the presence of sufficient liquid phase, making the contact between copper and freshly exposed silicon less probable. This is because the amount of fluorocarbon has to be kept low due to other potential spoiler reactions and due to the low density of fluorocarbon making it a nonideal transport medium. An additional liquid medium, lead acetate, melting point 280°C, was therefore chosen to transport copper grains to freshly exposed silicon sites. Liquid sintering of the copper matrix is still thought to be a solution growth phenomenon accomplished by the liquid metal lead.

The first paste containing lead acetate and fluorocarbon powder was F13 copper paste. The composition of this paste is given in Table 1 below.

Table 1 Composition of Paste F13

Material	Source	Amount (wt%)
Vehicle	Dupont	34.0
Fluorocarbon	Dupont	1.1
Aluminum-Silicon eutectic	Alfa-Ventron	1.1
Lead Acetate	Bakers	2.3
Lead Metal	MCB	4.6
Copper Metal	Colonial	56.9

3.0 Cont.

The paste was screened as a test pattern as well as solid electrode. During firing at a temperature of 556°C several variations of gas ambients were tried. The normal nitrogen-hydrogen two step firing gave reasonably good adherence, although some pulloff was observed in the Scotch tape test.

The two step firing process was described previously[3], but will be repeated in Table II for the sake of completeness.

Table II Two Step Firing Process

Time (minutes)	Gas	Wafer Temperature and Location
10	Nitrogen	∿25°C (Room temperature) outside furnace
3	Nitrogen	80°C - 150°C (dry) at furnace entrance
5	Nitrogen	at temperature (∿550°C) in furnace
8	Hydrogen	at temperature (∿550°C) in furnace
2	Hydrogen	550°C → 25°C (slow cool) to furnace exit
5	Hydrogen	Cool outside furnace
5	Nitrogen	Cool outside furnace

Best results were obtained in a run in which the sintering took place in nitrogen and hydrogen was used only during the cooling phase. A Scotch tape test (See Section 5) performed on the electrode from this run gave good results with virtually no pulloff.

Figure 4 and 5 show SEM micrographs of F13 electrodes fired at 550°C by the hydrogen cool process, with indicated magnifications. It can be seen that the degree of sintering is inadequate, and there is some evidence of oxidation in Figure 5. The two conditions may be related in that the lack of sintering may be due to lack of wetting by the liquid phase sintering

ORIGINAL PAGE IS
OF POOR QUALITY

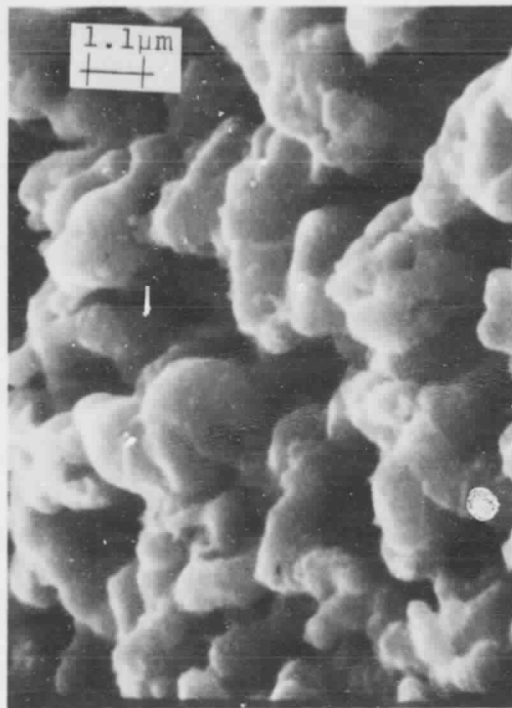

Figure 4. 1800x Figure 5. 9000x
SEM micrographs of F13, copper fluorocarbon electrode.

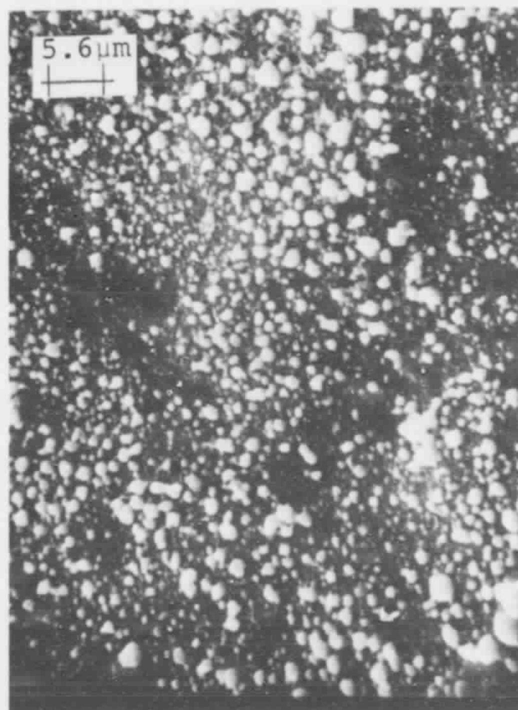

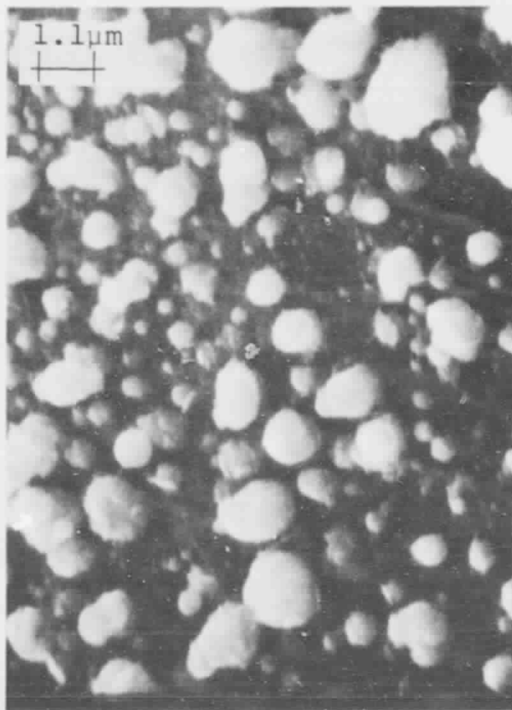

Figure 6. 1800x Figure 7. 9000x
SEM micrographs of substrates under above electrodes.

3.0 Cont.

medium (lead), since hydrogen is introduced only during cool-down. Figure 6 and 7 show SEM micrographs taken of substrates under F13 electrodes (525°C) after electrodes were removed mechanically. The white beads covering the surface appear to be dielectric in nature judging from the presumed charging effects of Figure 7. Therefore we believe the material to have resulted from the lead acetate and expect it to be lead oxide.

4.0 Paste and Contact Experimentation, Silver Fluoride

During the reporting period, six pastes using fluorocarbon and seven pastes using silver fluoride were fabricated. Most of these gave poor results, with powdery surfaces indicating inadequate sintering and insufficient adhesion. Figure 8 shows a microphotograph of a number of test pieces of early electrode paste samples. The Scotch tape strip for the adhesion test is displayed above each sample. Pastes are from top to bottom F5 (AgF), F6 (AgF) and F7 (fluorocarbon) and the firing temperatures are from left to right 525°C, 550°C, 575°C, 600°C and 625°C. In some cases the total electrode lifted from the substrate.

Since adhesion of the copper silver fluoride pastes was so poor, it was decided to try some of the original silver pastes (containing 2% silverfluoride), which had given excellent adhesion and scratch resistance. Silicon wafers were screened with silver ink S032 and fired at 550°C in air and by the two step process. Excellent adhesion was obtained in the case of airfired silver electrodes. Silver electrodes fired in hydrogen separated from the substrates spontaneously. The silver electrodes removed from the substrates had excellent sheet integrity and strength. The structure of the silver electrode sheets is shown in Figures 9 and 10 at 1800x and 9000x, respectively. The structure is so well interlocked as to appear oversintered. The smaller circular dots are believed to be a segregated metallic lead phase.

ORIGINAL PAGE IS
OF POOR QUALITY

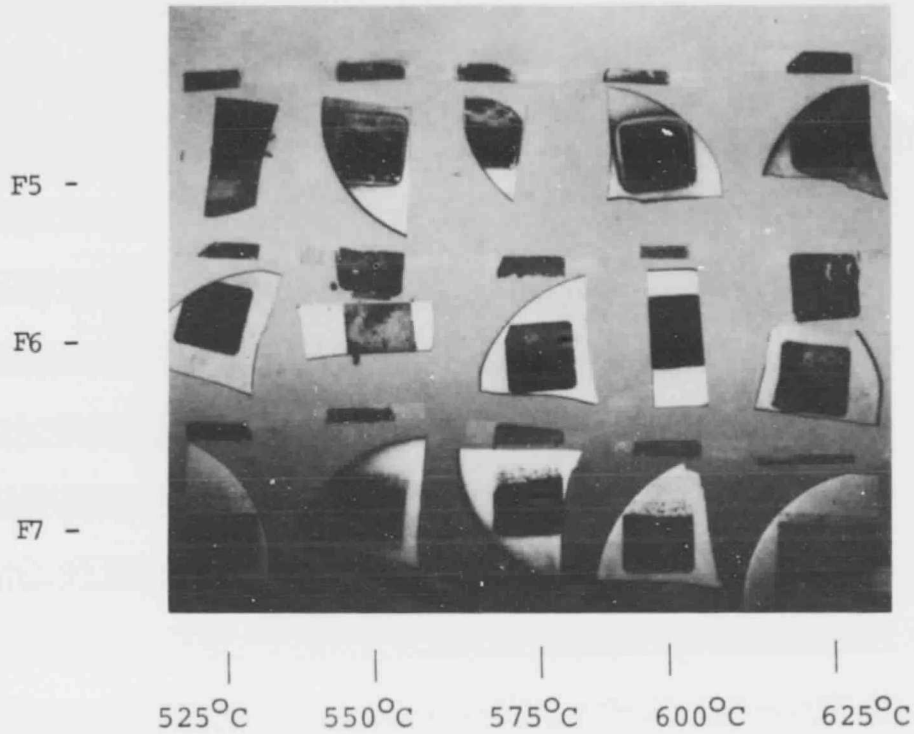

Figure 8. Photograph of 3 pastes with Scotch tape test strips above.

ORIGINAL PAGE IS
OF POOR QUALITY

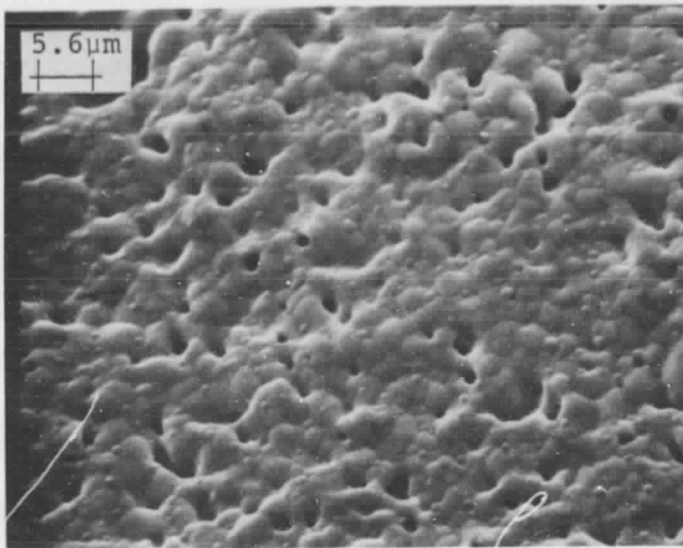

Figure 9. SEM micrograph of S032 silver electrode separated from silicon substrate, fired at 550°C by two step process at 1800x.

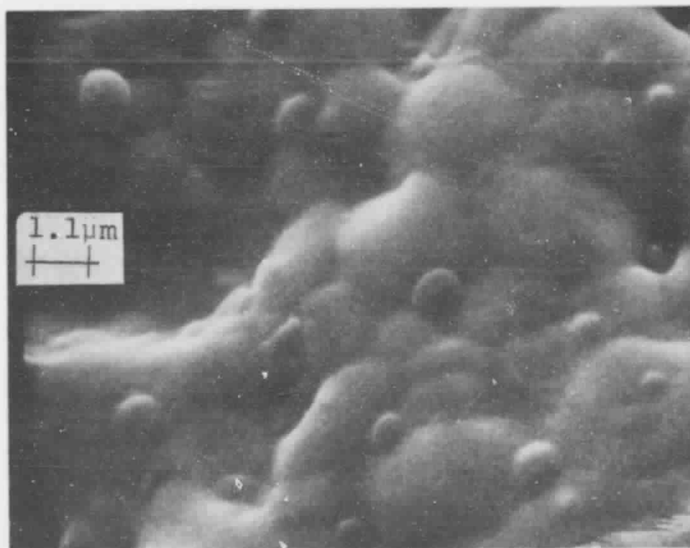

Figure 10. SEM micrograph of S032 silver electrode separated from silicon substrate, fired at 550°C by two step process at 9000x.

4.0 Cont.

Previously we suspected interference of the hydrogen with the etching action of the fluorine component. In view of the information obtained in Section 6.0, another explanation may be in order. The bonds at the silicon surface may be more attractive to hydrogen than other atomic species, based upon the remarkable silicon-hydrogen bond strength.

Silver fluoride content of the copper pastes ranged from 1.1 wt% to 3.7 wt%. Smaller quantities of silver fluoride were utilized after an analysis by Dr. Joseph Parker, which pointed to spoiler reactions resulting from the presence of silver fluoride.

The paste containing the smallest amount of silver fluoride gave the best results to date. One test sample fired in nitrogen at 550°C, passing the Scotch tape test (F12). Figures 11 and 12 show SEM micrographs of electrodes resulting from this experiment (shown at 1800x and 9000x, respectively) while the sintering action appears to be moderately good, the surface texture, suggests an oxide coating (particularly at the higher magnification).

One further variation tried was the use of copper flake for the major constituent in paste F15. Electrodes fired at 550°C by the two step process are shown as SEM micrographs in Figures 13 and 14. Magnifications are 1800x and 9000x, respectively. The electrodes resulting from this had good metallic sheen, presumably due to the orientation of the major flake plane, but poor adhesion and cohesion. In

ORIGINAL PAGE IS
OF POOR QUALITY

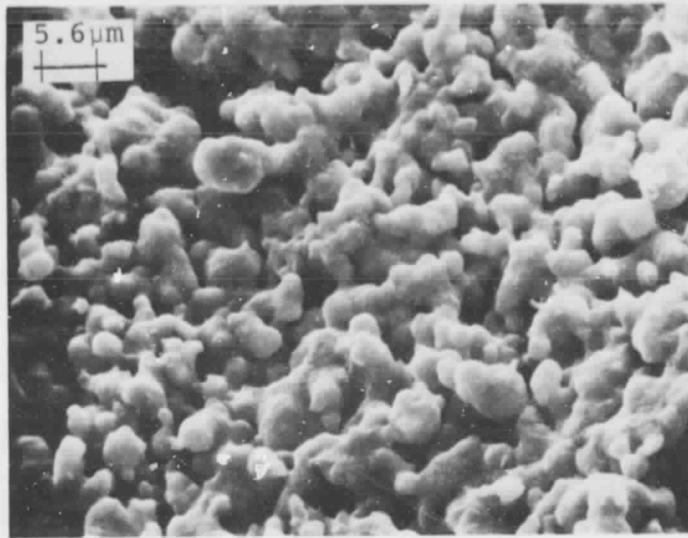

Figure 11. SEM micrograph of F12 electrode fired in nitrogen at 550°C, at 1800x.

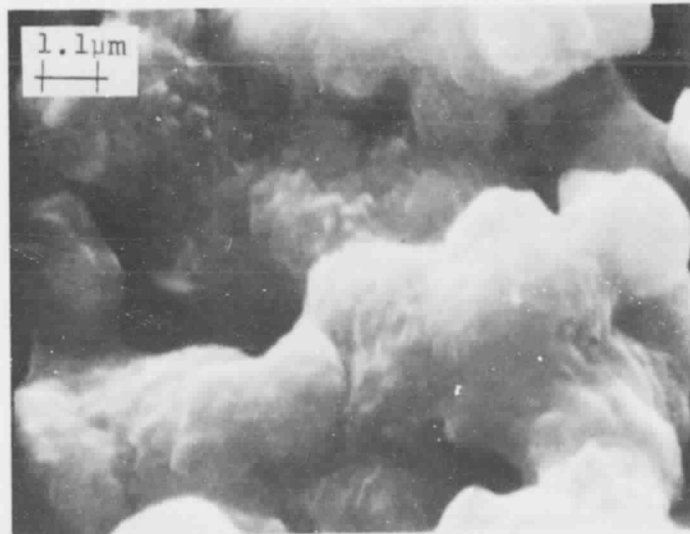

Figure 12. SEM micrograph of F12 electrode fired in nitrogen at 550°C, at 9000x.

ORIGINAL PAGE IS
OF POOR QUALITY

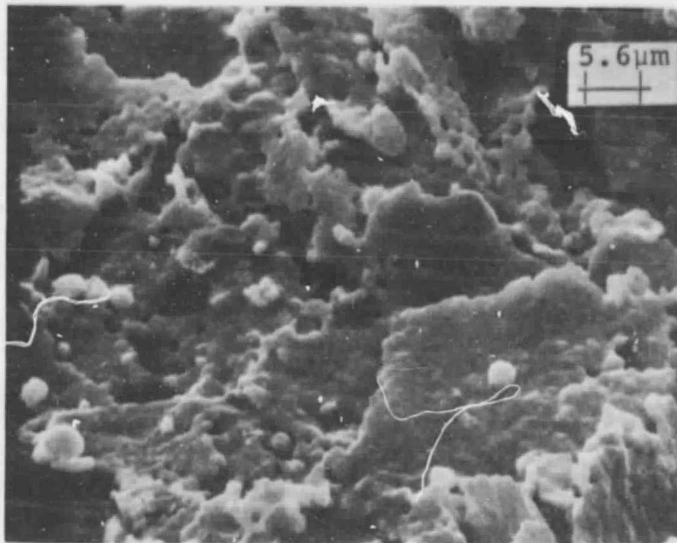

Figure 13. SEM micrograph of F15 copper paste with flake copper and silver fluoride, fired by the two step process at 550°C, at 1800x.

Figure 14. SEM micrograph of F15 copper paste with flake copper and silver fluoride, fired by the two step process at 550°C, at 9000x.

4.0 Cont.

addition, the flakes tended to coat the screen wire mesh.

S080 electrodes fabricated during a solar cell experiment under the previous contract[2] were reexamined. A fragment of a solar cell which originally had a copper contact applied with initially good adhesion, was found to have the contact partially separated. The electrode metal was curved away from the silicon substrate, indicative of strain, in the sense of contraction relative to the silicon. This is as would be expected from the thermal behavior of copper relative to silicon. The thermal expansion coefficients of copper, lead and silicon are, respectively:

$$\text{Copper} \quad \frac{1}{L}\frac{\partial L}{\partial T} = 17.71 \cdot 10^{-6} \; (^{\circ}C)^{-1}$$

$$\text{Lead} \quad \frac{1}{L}\frac{\partial L}{\partial T} = 28.9 \cdot 10^{-6} \; (^{\circ}C)^{-1}$$

$$\text{Silicon} \quad \frac{1}{L}\frac{\partial L}{\partial T} = 2.56 \cdot 10^{-6} \; (^{\circ}C)^{-1}$$

If appropriately sintered, a copper grain matrix exists at the end of the sintering step, which took place at 550°C in the subject device. The amount of strain resulting from the mismatch is 0.05 cm assuming the diameter of the solar cell to be 2.25 inches or 5.72 cm and the copper grain matrix to cool through 520°C without relaxation. The calculated radius of curvature of the electrode is 45.5 cm.

While the initial adhesion of S080 paste was excellent it appears that longterm storage (approximately 18 months) caused catastrophic spalling of the copper electrode.

4.0 Cont.

While the causes for this are not known, it may be that the relatively thick and densely sintered electrode could not withstand thermal cycling.

5.0 Results of Analysis

A simple Scotch[r] tape adherence test was devised to allow crude, instant evaluation of the results of electrode tests. Likewise a scratch test, that allows comparative analysis of the electrode strength, was initiated.

During the present reporting period a number of pastes manufactured previously with varying parameters were analyzed. The manual screening was improved to allow reproducible registration and constant snapoff distance (.012"). The tube furnace was reprofiled with the standard platinum - platinum plus 13% rhodium thermocouple and a digital microvoltmeter. An error was found on the furnace chromel-alumel thermocouple. Spot checks with platinum reference thermocouple were made routine on all firings. Some variation in firing was found leading to some suspicion of potential downstream contamination from contaminated furnace tube, gas or exudant from upstream samples.

Problems with layers were:

1) Lack of adhesion, possibly due to inadequate reduction of oxide, (silicon surface and powder grain surfaces) or tying up of dangling surface bonds by hydrogen atoms.
2) Poor sintering due to inadequate liquid transport (discussed in Section 3.0).

Samples of characterization attempts of successful and unsuccessful pastes are shown in the following figures. Figure 15 depicts four optical photomicrographs of successful S080 substrates (upper left) and S080 print (upper right) and unsuccessful S079 substrate (lower left)

ORIGINAL PAGE IS
OF POOR QUALITY

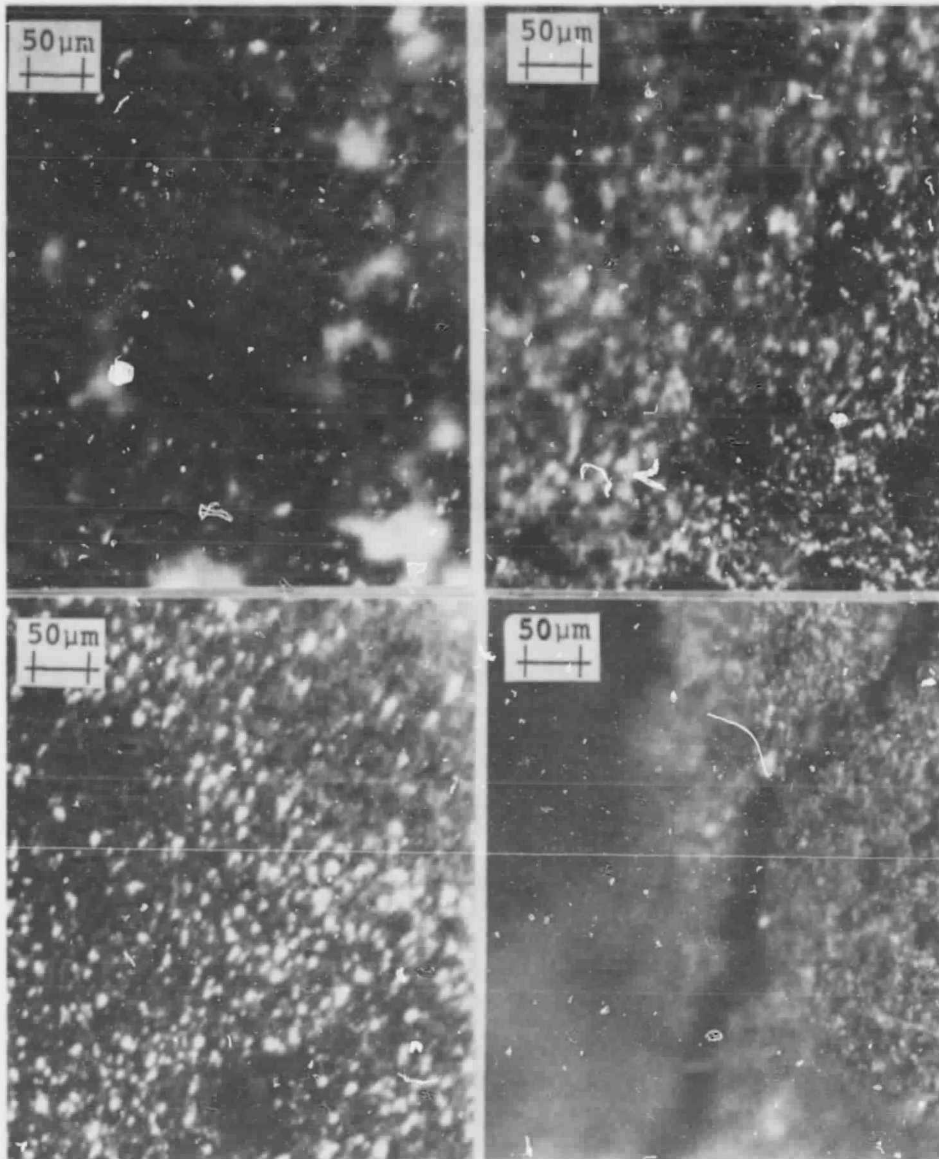

Figure 15. Optical micrographs of S080 successful and S079 unsuccessful screened prints with experimental copper pastes.
LEFT SIDE, TOP: Silicon substrate under good S080 print (Electrode removed by acid etch).
BOTTOM: Silicon substrate of S079 print (electrode peeled spontaneously).
RIGHT SIDE, TOP: S080 successful electrode print.
BOTTOM: S079 unsuccessful electrode print.
Magnification 200X

5.0 Cont.

and S079 print (lower right). In the case of the substrates the S080 electrode was removed by etching with concentrated nitric acid, and the S079 electrode print peeled spontaneously. The difference between S080 and S079 is the use of germanium-silicon eutectic at 5wt.% in the former and aluminum-silicon eutectic in the latter.

The major observable difference in the micrographs is the larger grain size and coarser faceting in the case of the successful S080 paste.

Figure 16 shows a composite of SEM micrographs depicting an unsuccessful S080 electroding experiment. The substrate is shown on the left side and the electrode on the right, both at 1800x and at 4500x. The firing of this paste at 550°C by the two step process resulted in a small degree of sintering, making the micrograph resemble that of a powder.

By contrast, Figure 17 shows a successful print of the S080 paste taken on a Cambridge SEM at roughly two magnifications 1800 - 1900x, and 4500 - 4700x. The striking appearance of the copper silicon eutectic needle structure dominates the pictures of the silicon substrate. On the right the electrode can be seen.

Figures 18 and 19 show black and white reproductions of the color readout of xray dispersive spectra of successful S080 electrodes and the silicon substrate, respectively. The spectra allow reading of the lines of copper (Cu), Aluminum

ORIGINAL PAGE IS
OF POOR QUALITY

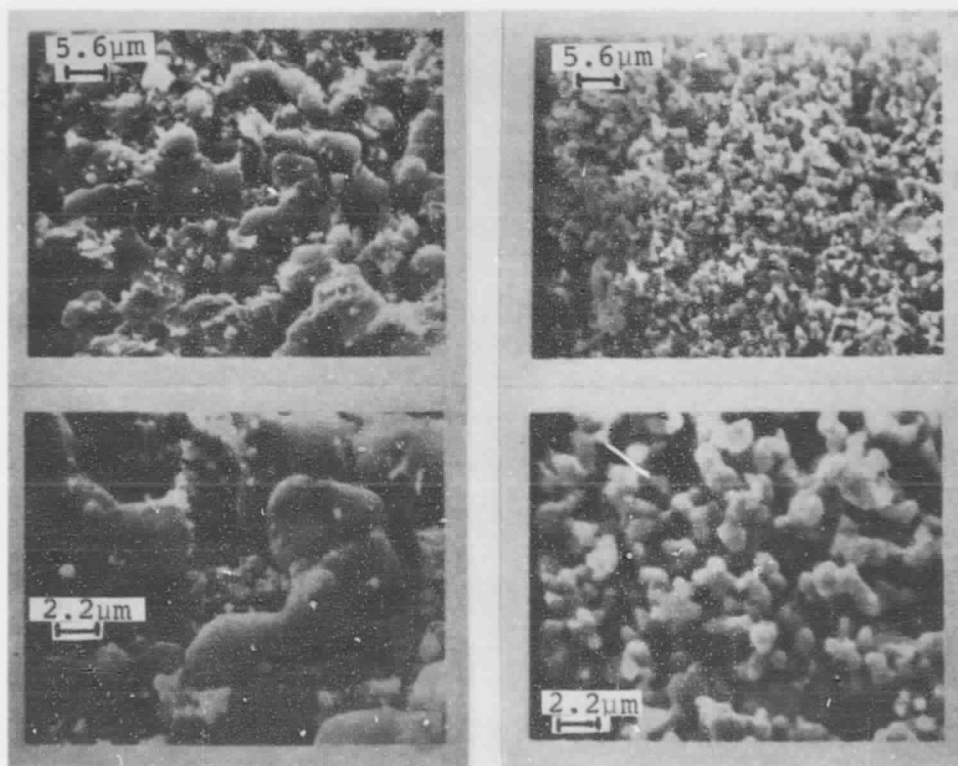

Figure 16. Composite of SEM micrographs of S080 unsuccessful electroding experiment.
Left Side: Substrate.
Right Side: Electrode.

ORIGINAL PAGE IS
OF POOR QUALITY

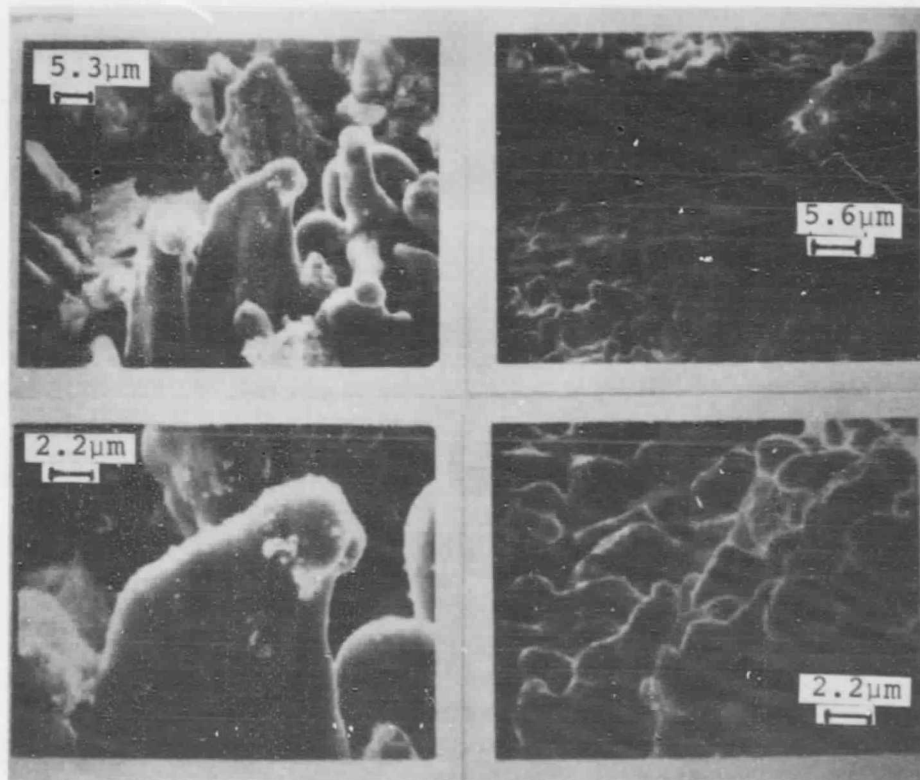

Figure 17. Composite of SEM micrographs of S080 successful screen print.
Left Side: Silicon substrate.
Right Side: Electrode.

ORIGINAL PAGE IS
OF POOR QUALITY

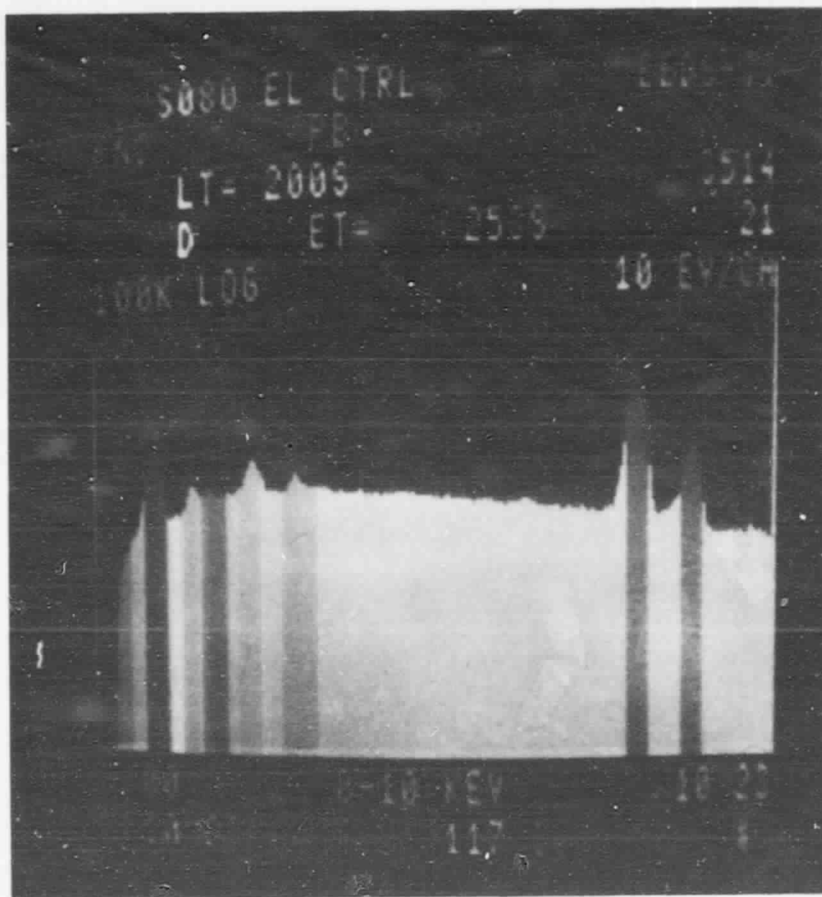

Figure 18. Black and white reproduction of color coded Xray dispersive spectrum of successful S080 electrode.

ORIGINAL PAGE IS
OF POOR QUALITY

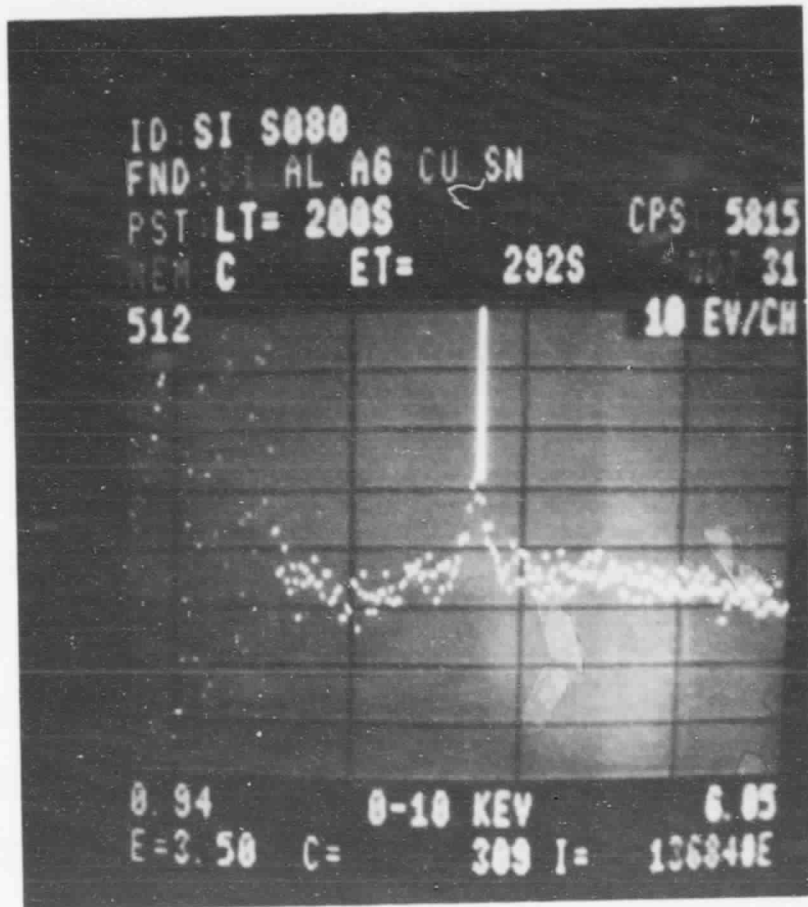

Figure 19. Black and white reproduction of color coded Xray dispersive spectrum of successful S080 electrode.

5.0 Cont.

(Al), lead (Pb) silicon (Si) and silver in Figure 18 and silicon, aluminum silver, copper and the (Sn) in Figure 19. The figures are shown only as illustrative of the method, as no clues for the differences in performance could be obtained from the spectra.

6.0 Information Exchange with German R&D Labs and PVSEC

During the month of October, two Siemens facilities in Munich, Germany were visited. At the semiconductor device plant at Frankfurter Ring, Drs. K. Reuschel and K. Platzöder were met and device processing was discussed.

The Wacker-Chemie plant at Burghausen, Bavaria, Mr. Vieweg-Gutberlet was also visited and silicon material properties (minority carrier lifetime and defect phenomena) were discussed.

The Solid State Institute (IFT) of the Fraunhofer-Gesellschaft was visited and contact problems, as well as minority carrier lifetime measurements were discussed with Dr. H. Sigmund.

Siemens Research Labs, Neu-Perlach was visited on two occasions and solar cell research (Siemens' amorphous sputtering and evaporation approach) were discussed, as well as contact problems, minority carrier lifetime measurement and other activities. Research lab personnel interviewed were Drs. G. Winstel, J.G. Grabmaier, E.F. Krimmel, Patalong, M. Möller, R.D. Plättner and Herberg.

Several papers were obtained from the Siemens group. One of these discussed the strong attachment of hydrogen to the dangling bonds in amorphous silicon material. Quoting the reference "The most striking feature shown by these measurements is however the great bond strength of the hydrogen in the a-Si:H,Cl network up to very high temperatures. Only at temperatures of about 1000°K do perceptible

6.0 Cont.

amounts of hydrogen escape, which may be due to recrystallization setting in at this temperature.[4] Since the surface of crystalline silicon has dangling bonds, similar to the amorphous material, this may help explain the displacement of silver and copper observed at high temperatures in hydrogen ambients. This phenomenon is discussed in further detail in the appropriate section.

7.0 Conclusions and Problems

Screened electrodes made from F13 (fluorocarbon activated copper paste) and F12 (silver fluoride activated copperpaste) were the first samples during this contract period which passed tape adhesion and scratch tests.

During firing tests it was found that:

a) nitrogen firing resulted in severely oxidized copper grains

b) the position of silicon wafers (standing in slotted boat or lying flat) had a bearing on the results

c) the duration of the second step (hydrogen flow) in the two step firing was a factor in the adherence of the electrode to the silicon substrate

Several explanations are possible for this behavior. Contamination of the flow gases was ruled out, since it was verified that all nitrogen procured, since firing first commenced, was oil pumped (vs. water pumped), and no other evidence pointed in that direction. However, back streaming, convective flow and therefore air contamination of furnace atmosphere in the open exit quartz tube was considered likely.

Evidence exists for the saturation of dangling bonds at the silicon surface by hydrogen during the sintering step.

Further contamination of furnace quartz furniture was another possibility and was therefore assumed. Mechanical problems with roller adjustability and paste throwing of the three roll mill were found.

ORIGINAL PAGE
BLACK AND WHITE PHOTOGRAPH

8.0 Plans and Recommendations

Further experiments with paste parameter variations and firing parameter variation will be done.

The tube furnace and associated gas handling equipment will be moved from the present marine dominated climatology with probable aerosol salt powder contamination to a location approximately 8 miles further inland.

Also, the following steps are to be taken during the next period to counter the reported problems:

1) Convection and backstreaming will be reduced by insertion of an alumina fiber plug into the quartz tube exit during firing. This alumina plug is to restrict the exit diameter, break up the gas stream into a number of small filamentary streams and increases the velocity of the streams, thereby reducing backdiffusion.
2) All quartz furniture will be taken to a professional glass shop for cleaning.
3) The three roller mill will be repaired and roller speed will be reduced.

Further analysis of the chemical reactions backed by differential thermal analyses as well as thermal gravimetric analyses are planned.

Finally, solar cell experiments will be made with the recent promising contact pastes, including some containing fluorocarbon powder.

9.0 References

1. B. Ross, Extension Final Report, "Production Process and Equipment Development" DOE/JPL 955164-79/4, p. 10 (Dec. 1979)

2. Ibid, p. 72

3. Ibid, p. 60

4. R.D. Plättner, W.W. Kröhler, B. Rauscher, W. Stetter and J.G. Grabmaier, Proc. 2nd E.C. Photovoltaic Solar Energy Conference, p. 860, Berlin W, (April 1979)

10.0 Progress on Program Plan

PROGRAM ACTIVITY	MONTHS AFTER AWARD												
	1	2	3	4	5	6	7	8	9	10	11	12	13
Cu Metallization (A)	▽			△									
Metallization (B)			▽			△							
Metallization (C)					▽				△				
Metallization (D)							▽				△		
Analysis and Test	▽											△	
Cell Delivery											•		
Cost Analysis - SAMICS											•		
Reports - Monthly		X	X		X	X			[illegible]		•		
- Quarterly				X			X			X			
- Final											•		
Review Meetings			X		X		X		X			•	•
Project Integration Meetings	X					X				•			
Project Workshops	As Specified by JPL												

▽ Start

△ Complete

• Proposed

X Completed